Supporting Information

An interfacial crosslinking strategy to fabricate an ultrathin two-dimensional composite of silicon oxycarbide-enwrapped silicon nanoparticles for high-performance lithium storage

Junlong Huang, Kunyi Leng, Yongqi Chen, Luyi Chen, Shaohong Liu, Shaukat Khan, Dingcai Wu and Ruowen Fu*

Materials Science Institute, PCFM Lab and GDHPRC Lab, School of Chemistry, Sun Yat-sen University, Guangzhou 510275, China

Email: cesfrw@mail.sysu.edu.cn

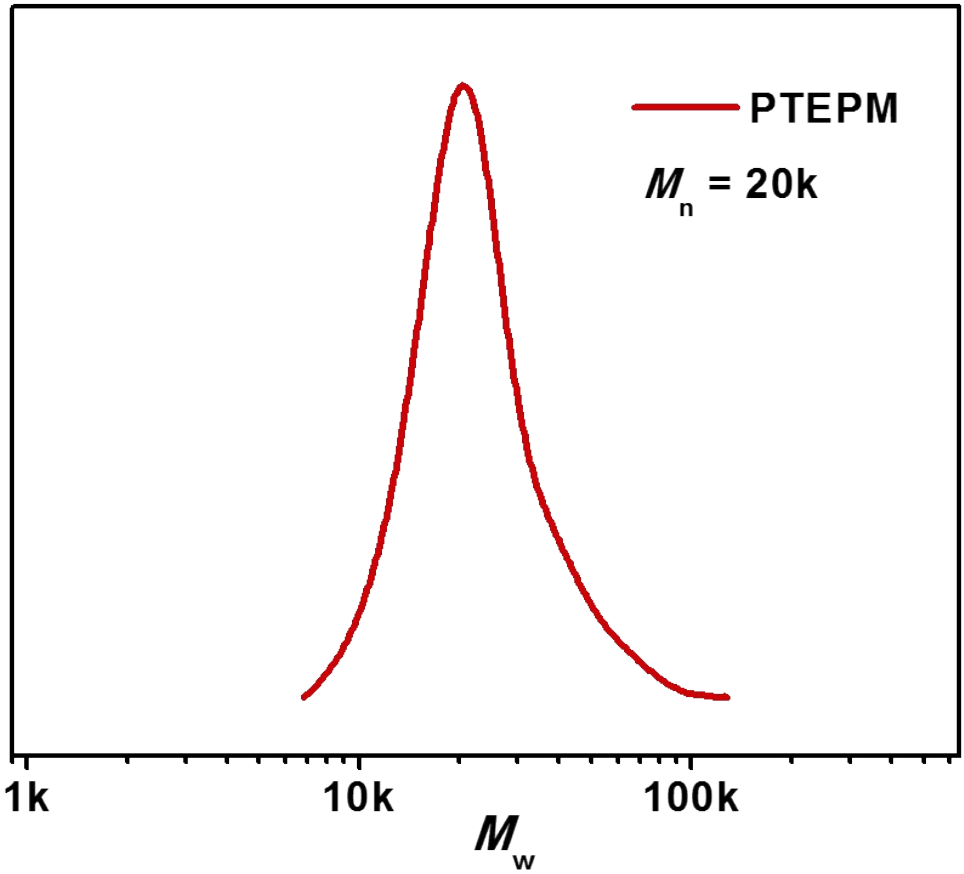

Fig. S1 Molecular weight distribution curve of PTEPM.

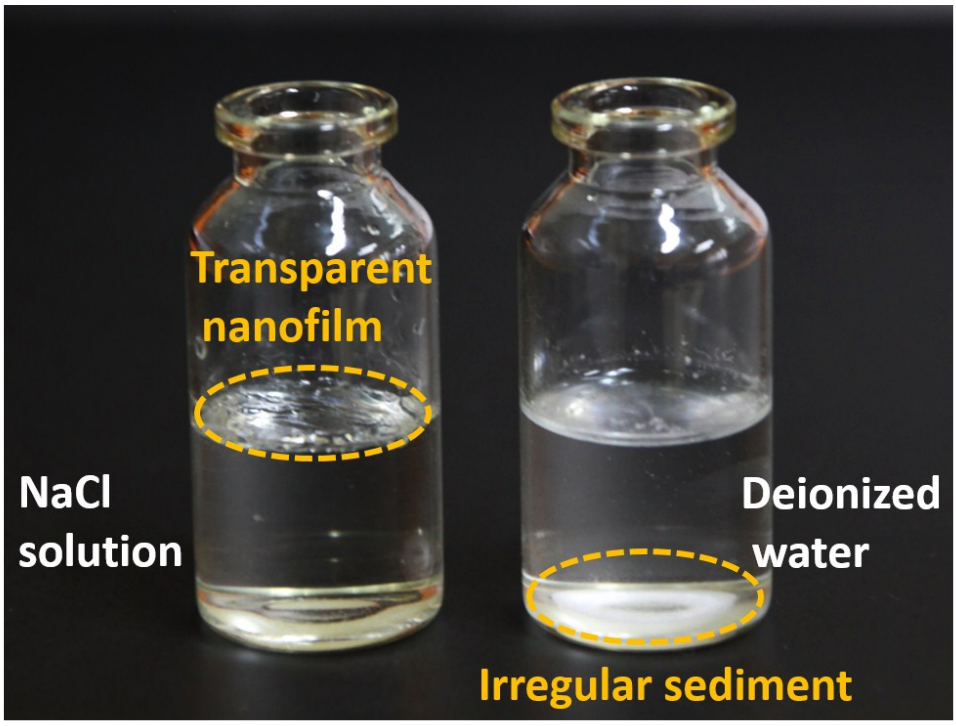

Fig. S2 Comparison of digital photos of PTEPM solutions precipitated in saturated NaCl solution (left) and deionized water (right).

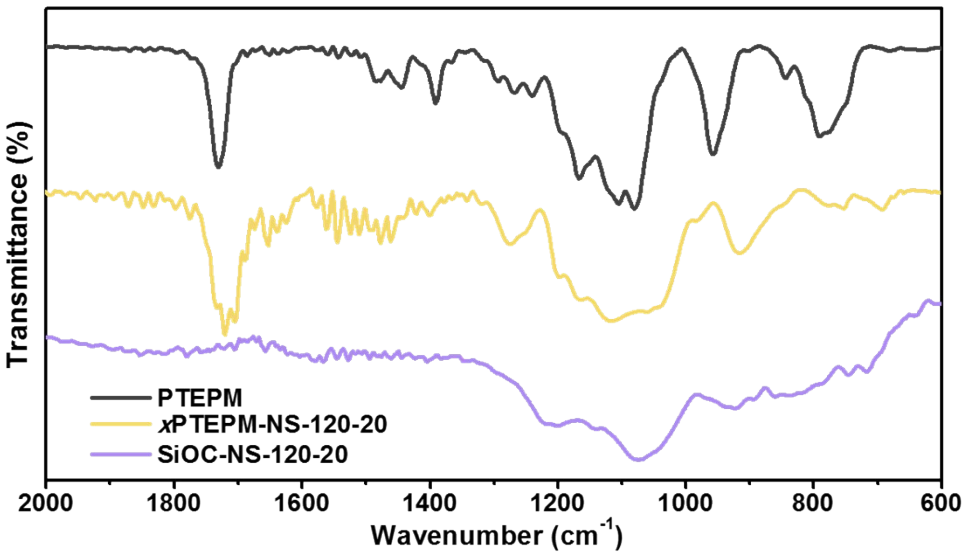

Fig. S3 FT-IR spectra of PTEPM, xPTEPM-NS-120-20 and SiOC-NS-120-20.

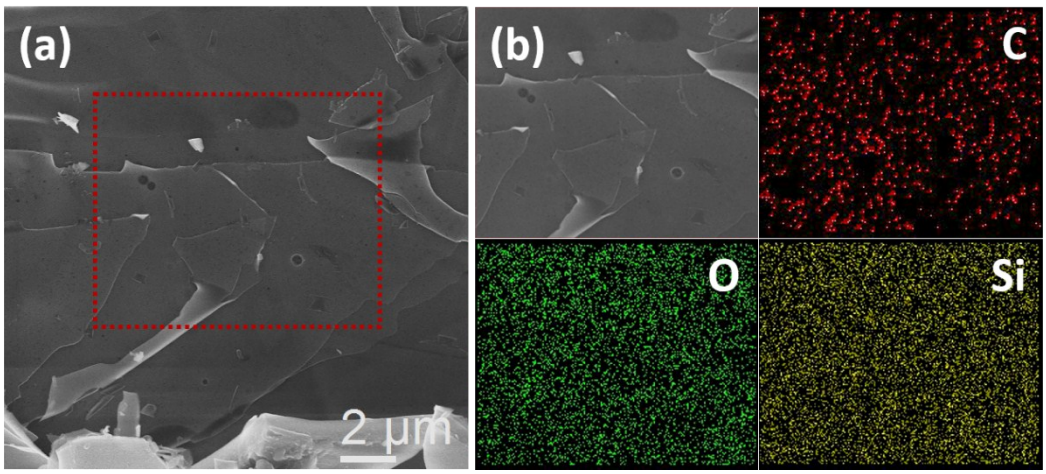

Fig. S4 SEM image of SiOC-NS-120-20 and the corresponding EDX elemental mappings of C, O and Si.

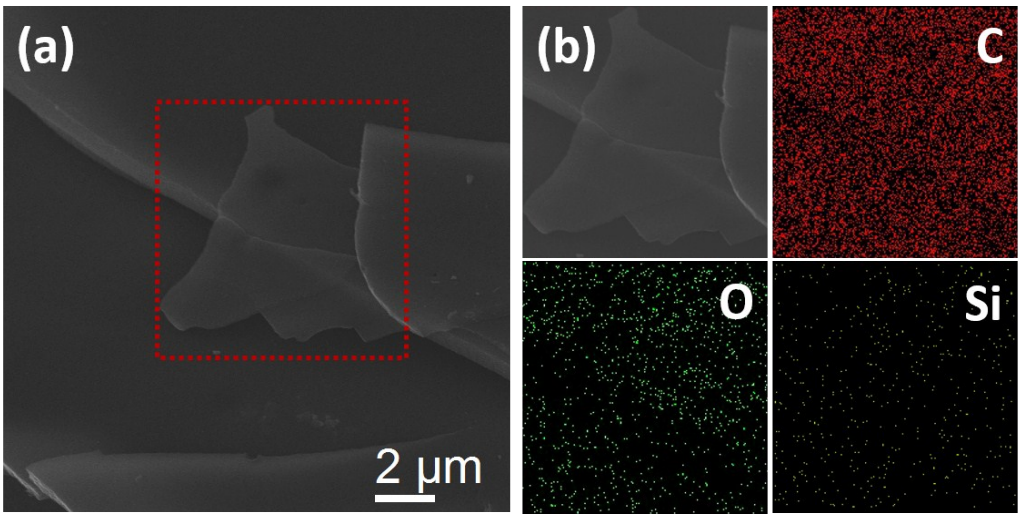

Fig. S5 SEM image of C-NS and the corresponding EDX elemental mappings of C, O and Si.

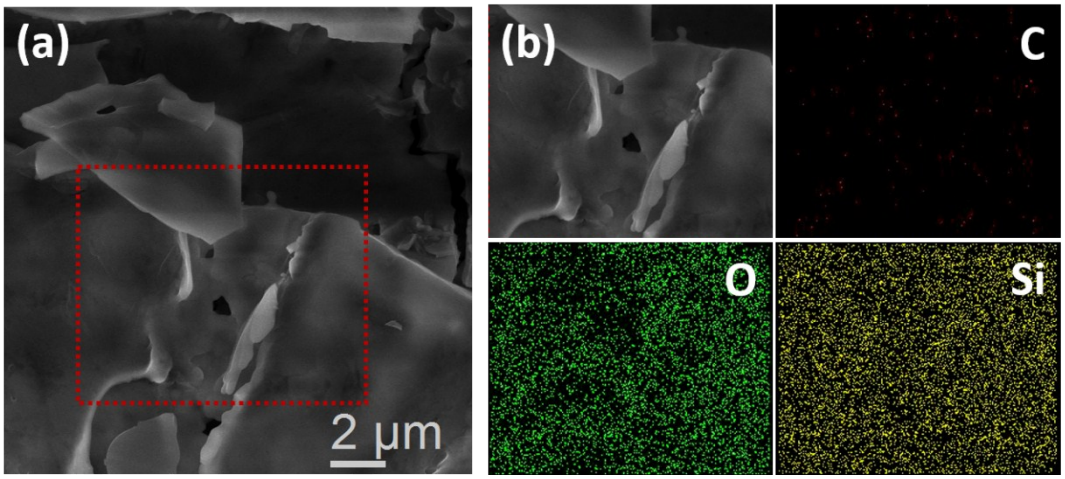

Fig. S6 SEM image of SiO_2-NS and the corresponding EDX elemental mappings of C, O and Si.

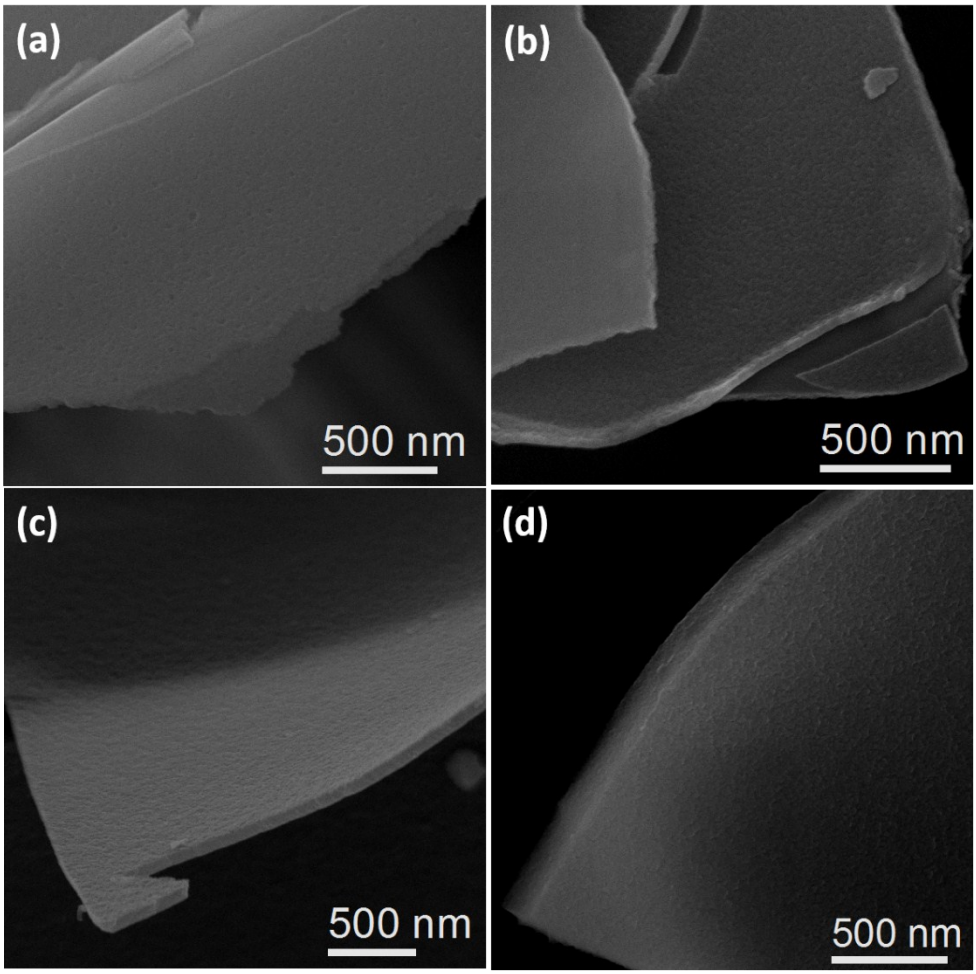

Fig. S7 SEM images of (a) SiOC-NS-30-5, (b) SiOC-NS-120-5, (c) SiOC-NS-120-20 and (d) SiOC-NS-120-50.

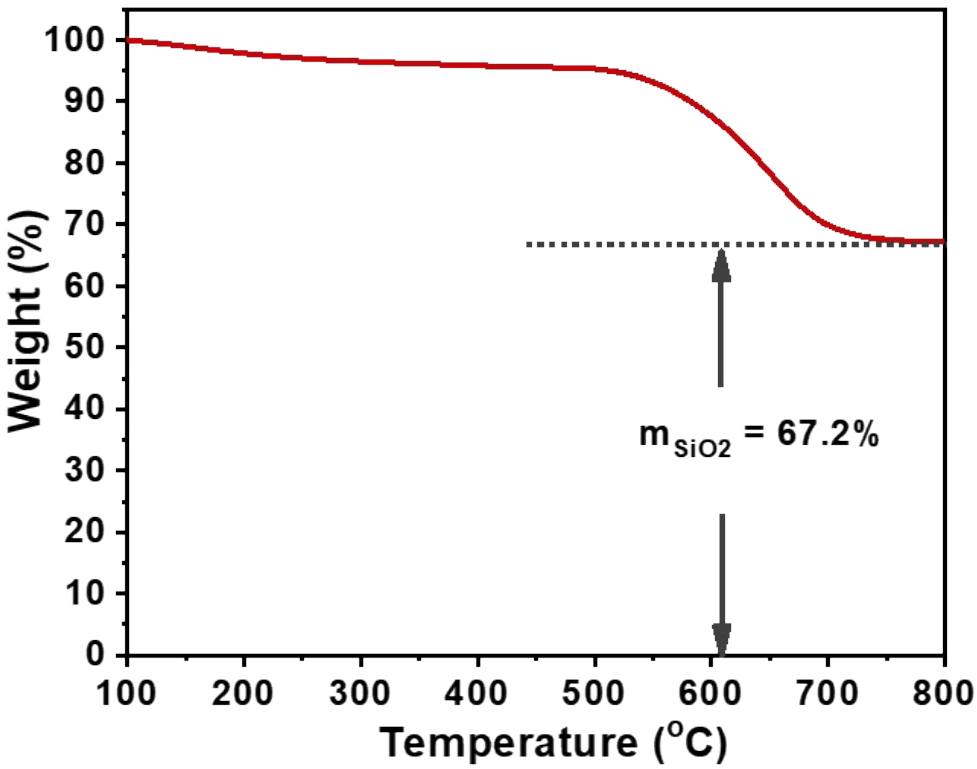

Fig. S8 Thermogravimetric analysis curve of Si/SiOC-NS.

Since the TGA test was carried out under O_2 atmosphere, the siliceous components were ultimately oxidized to SiO_2. According to the TGA result, the mass ratio of SiO_2 (m_{SiO2}) was 67.2%. According to the XPS analysis of high-resolution Si 2p spectrum, the mass ratio of Si (m_{Si}) in Si/SiOC-NS can be calculated as follow:

$$m_{Si} = \frac{m_{SiO2}}{M_w(SiO_2)} * A_{Si} * M_w(Si) = \frac{67.2\%}{60} * 0.244 * 28 = 7.7\%,$$

where the $M_w(SiO_2)$, $M_w(Si)$ and A_{Si} represent the molecular weight of SiO_2, Si and atomic percentage of Si, respectively. Thus, the mass ratio of Si to SiOC in the Si/SiOC-NS can be defined to be 7.7: 92.3.

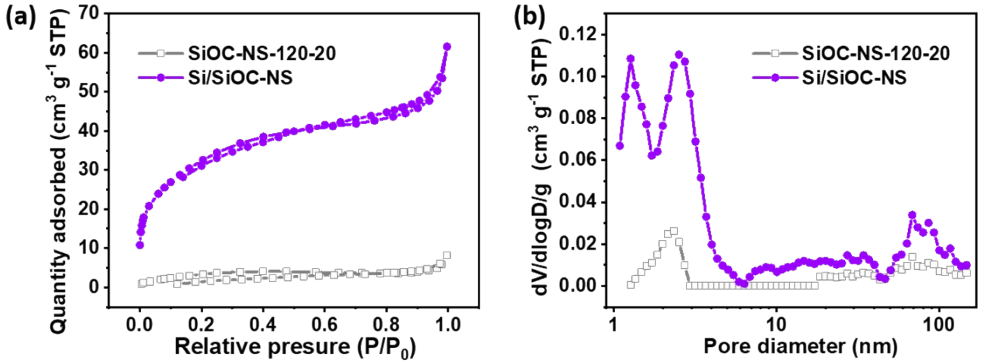

Fig. S9 (a) N_2 adsorption–desorption isotherms and (b) DFT pore size distribution curves of SiOC-NS-120-20 and Si/SiOC-NS.

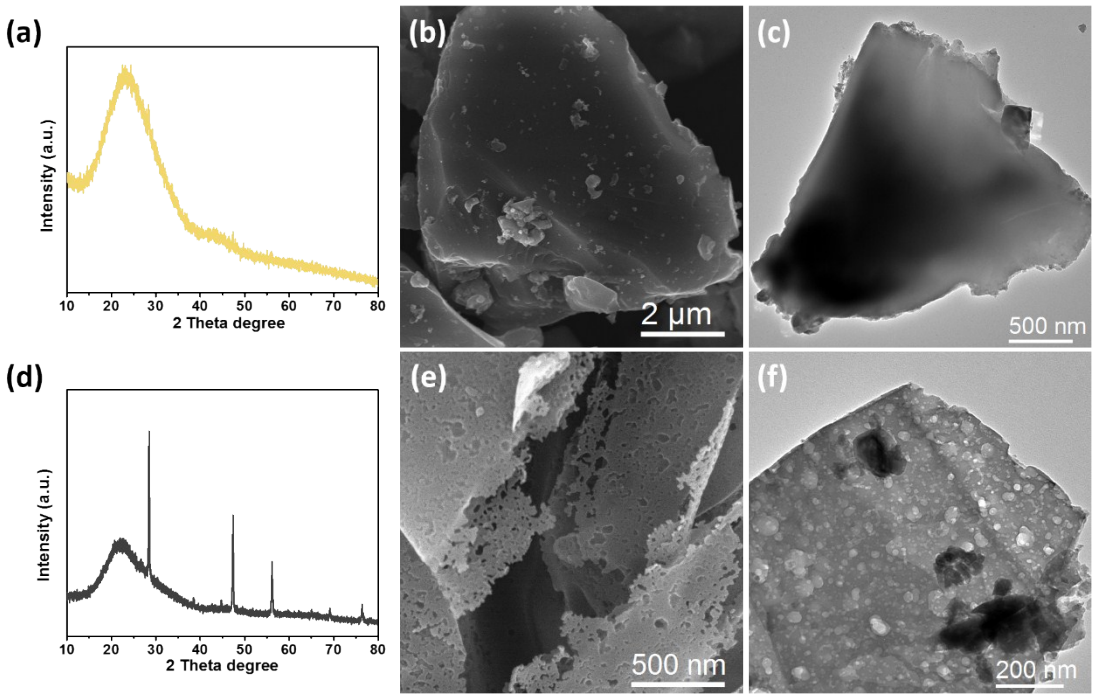

Fig. S10 (a, d) XRD patterns, (b, e) SEM images and (c, f) TEM images of (a, b and c) Si/SiOC-M and (d, e and f) Si/SiO_2-NS.

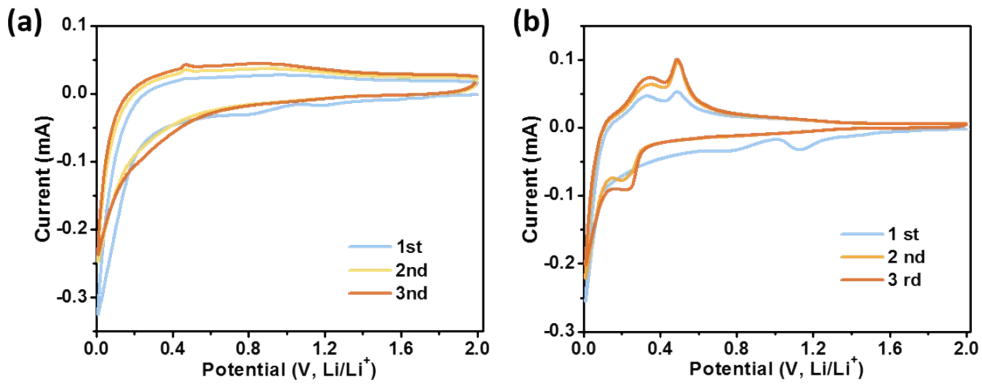

Fig. S11 CV curves of (a) Si/SiOC-M and (b) Si/SiO_2-NS electrodes at a scan rate of 2 mV s^{-1}.

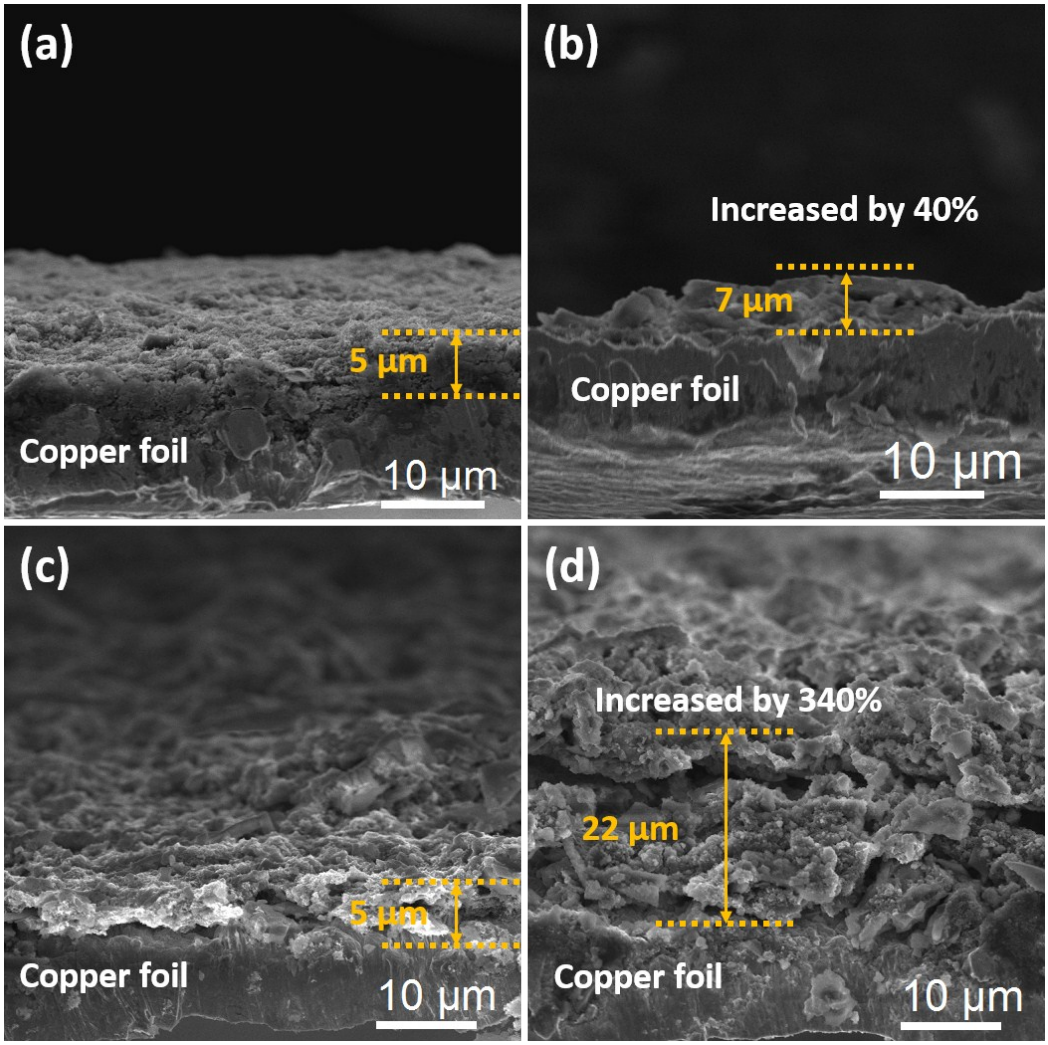

Fig. S12 Cross-sectional SEM images of (a, b) Si/SiOC-NS electrode and (c, d) Si/SiO_2-NS electrode (a, c) before and (b, d) after cycling at 1 A g^{-1} for 100 cycles.

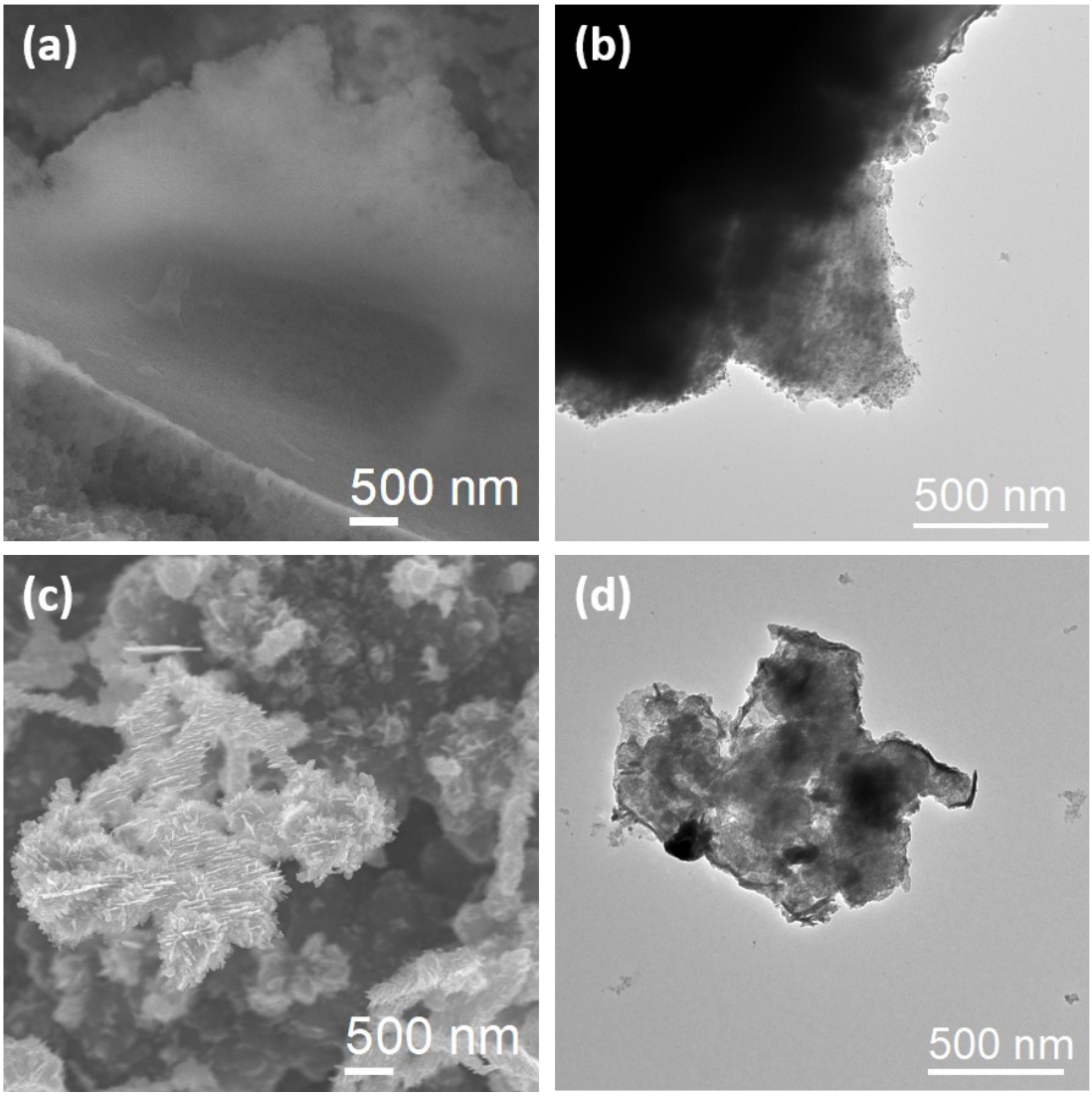

Fig. S13 (a, c) SEM and (b, d) TEM images of (a, b) Si/SiOC-NS and (c, d) Si/SiO_2-NS after cycling at 1 A g^{-1} for 100 cycles.

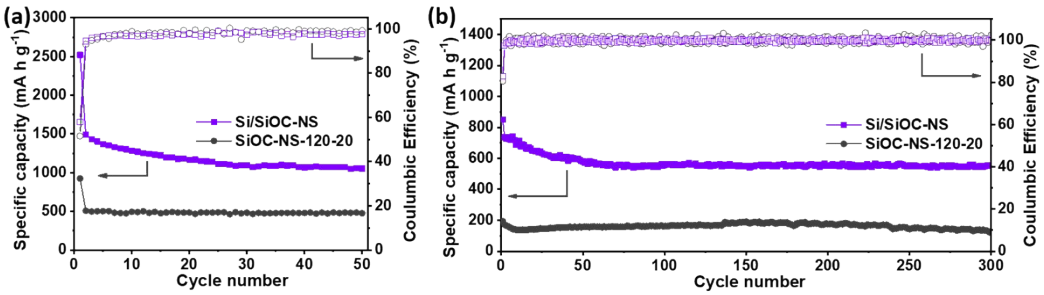

Fig. S14 Cycling performances and Coulombic efficiency of the Si/SiOC-NS and SiOC-NS-120-20 electrodes (a) at 0.2 A g^{-1} and (b) 5 A g^{-1}.

Table S1. A comparison of electrochemical properties between Si/SiOC-NS and other Si-based anode materials.

Active materials	Electrochemical properties	References
Si/SiOC-NS	**486-1234 mA h g^{-1} at 0.1-5 A g^{-1}**	**This work**
SiOC particles supported by reduced graphene oxide (SiOC/GO)	543-620 mA h g^{-1} at 0.1-2.4 A g^{-1}	S1
Si confined in SiO_2 and coated with carbon (nano-Si/*a*-SiO_2@C)	648-980 mA h g^{-1} at 0.15-1.5 A g^{-1}	S2
Mesoporous Si coated with carbon (mpSi-Y/C)	260-1150 mA h g^{-1} at 0.1-5 A g^{-1}	S3
Si connected with mesocarbon microbeads and coated with carbon (MCMB@Si@C)	490-900 mA h g^{-1} at 0.1-1.6 A g^{-1}	S4
Monodisperse SiO_x/C microspheres (SiO_x/C)	620-870 mA h g^{-1} at 0.1-0.6 A g^{-1}	S5
Yolk@shell structured SiO_x/C (SiO_x/C-CVD)	410-1100 mA h g^{-1} at 0.1-5 A g^{-1}	S6
Si dispersed in SiOC nanosphere (Si/SiOC)	303-880 mA h g^{-1} at 0.1-5 A g^{-1}	S7

Table S1 Fitted impedance parameters of samples

Parameter	Si/SiOC-NS	Si/SiOC-M	Si/SiO_2-NS
R_o /Ω	8.674	8.19	3.933
R_{ct} /Ω	70.03	45.05	152.8
CPE /μF	38.41	19.35	51.83
W_o /Ω	11.02	22.14	19.23

Reference

S1. L. David, R. Bhandavat, U. Barrera and G. Singh, *Nat. Commun.*, 2016, **7**, 10998-11008.

S2. R. Fu, K. Zhang, R. P. Zaccaria, H. Huang, Y. Xia and Z. Liu, *Nano Energy*, 2017, **39**, 546-553.

S3. N. Kim, H. Park, N. Yoon and J. K. Lee, *ACS Nano*, 2018, **12**, 3853-3864.

S4. Y. Lin, Y. Chen, Y. Zhang, J. Jiang, Y. He, Y. Lei, N. Du and D. Yang, *Chem. Commun.*, 2018, **54**, 9466-9469.

S5. Z. H. Liu, D. D. Guan, Q. Yu, L. Xu, Z. C. Zhuang, T. Zhu, D. Y. Zhao, L. Zhou and L. Q. Mai, *Energy Storage Materials*, 2018, **13**, 112-118.

S6. Z. H. Liu, Y. L. Zhao, R. He, W. Luo, J. S. Meng, Q. Yu, D. Y. Zhao, L. Zhou and L. Q. Mai, *Energy Storage Materials*, 2018, **19**, 299-305.

S7. Z. Wu, W. Q. Lv, X. Q. Cheng, J. L. Gao, Z. Y. Qian, D. Tian, J. Li, W. D. He and C. H. Yang, *Chem. Eur. J*, 2019, **25**, 2604-2609.